J Mater Sci (2019) 54:4484–4494

Ceramics

Porous Si_3N_4-based ceramics with uniform pore structure originated from single-shell hollow microspheres

Xiaoyan Zhang[1], Wenlong Huo[1,*], Yuju Lu[1], Ke Gan[1], Shu Yan[1], Jingjing Liu[1], and Jinlong Yang[1,*]

[1] *State Key Lab of New Ceramics and Fine Processing, School of Materials Science and Engineering, Tsinghua University, Beijing 100084, China*

Received: 25 July 2018
Accepted: 7 November 2018
Published online: 5 December 2018

ABSTRACT

Herein, the advantage of single-shell hollow microspheres on forming pores has been exploited to acquire porous ceramics with homogeneous microstructure, while the hollow microspheres also acted as reaction source. Dispersant reaction method has been applied to realize the perfect combination between microspheres and Si_3N_4 particles, which could be attributed to the repulsion between particles is weakened, particles agglomerate together and holding microspheres among them tightly. Owing to the normal distribution of hollow spheres and their single-shell structure, porous Si_2N_2O-Si_3N_4 ceramics with uniform pore distribution have been fabricated. The results show that the addition of silica hollow spheres contributes to the decrease in dielectric constant, since their porosity could be increased effectively and Si_2N_2O phase exhibiting low dielectric constant is generated. High-performance porous Si_3N_4 ceramics with porosity of 45.7% have been prepared through employing fly ash hollow microspheres, which possess flexural strength of 108.76 ± 6.25 MPa, fracture toughness of 1.78 ± 0.09 MPa $m^{1/2}$ and dielectric constant of 3.53. This strategy is proved to be a convenient, eco-friendly and effective method to synthesize ideal candidates for radomes.

Introduction

Due to their unique structure, especially internal free space and the shell creating isolated environments, hollow spheres with large surface area and high permeability display special mechanical, optic, thermal, electromagnetic, acoustic and catalytic properties [1]. Accordingly, their applications in energy storage field, photocatalytic degradation of organic pollutants in water, controlled release of drugs, protection of light-sensitive components and gas sensing devices have been attracted more and more attention in recent years [2–5]. Apart from meeting the requirements of functional applications, hollow spheres have become one of the most common additives to prepare structural ceramic components

Address correspondence to E-mail: huowenlong1991@163.com; jlyang@mail.tsinghua.edu.cn

https://doi.org/10.1007/s10853-018-3118-2

for specific purpose, especially for porous ceramics [6–8]. In comparison with general pore formers, ceramic hollow spheres show good sphericity and monodispersion, which are more convenient to be operated mainly because the binder removal process could be avoided and it is easier to fabricate porous ceramics with well adjustable pore structure and porosity [9].

So far, porous ceramics from hollow spheres could be generally divided into two major routes, namely bonding hollow spheres together and adding hollow spheres into suspension as pore-forming agents. The former approach is commonly used since it is simple, low cost, flexible, convenient and easy to operate. Either the internal space of hollow spheres or the gaps among the hollow spheres could well supply pores for the final products. Therefore, hollow spheres are commonly used as the skeleton structure and coated with ceramic slurry to achieve porous structure, while their sintering properties are exploited to realize the bonding of shells from hollow spheres, even with the aid of high-temperature binder [10, 11]. In these cases, various ceramic foams have been proposed based on hollow microspheres, and their unique three-dimensional porous structure brings prominent applications in filters and thermal insulators [12]. Nevertheless, the mechanical strength of products is the major problem needed to be solved in this method, especially for the weaker junction between hollow spheres and the effects of relatively high porosity caused by this approach, which could be well avoided in the latter route.

In regard to porous ceramics employing hollow spheres as pore former in combination with given slurry, the dispersity of added hollow spheres in suspension and their combination with matrix after forming and drying process become the major problems needed to be solved. In our previous work, poly-hollow microspheres, fabricated in large scale via spray drying particle-stabilized foam suspensions [13], are used to fabricate various porous ceramics for thermal insulators, wave-transparent material and acoustic absorption applications [14]. However, subjected to the weak combination between hollow spheres and matrix, the mechanical properties of prepared porous ceramics are less favorable [15]. Different from poly-hollow microspheres, single-shell hollow microspheres possess completely empty cavity, providing sufficient condition for adjusting pore structure of the final porous ceramics merely by selecting different amounts or particle size distributions of hollow microspheres. In addition, single-shell structure enables the complete reaction between hollow spheres and their surrounded matrix or coating to realize the effects of enhancement or modification. As is well known that porous ceramics with excellent microstructure reflected in uniform pore distribution, small pore size and more spherical pore morphology could endow them with outstanding mechanical strength, thermal and dielectric performances [16–20]. Apparently, hollow spheres with single-shell structure could better achieve the optimization of porous structure, which is rarely reported.

Among various applications for porous ceramics, including gas/liquid filters [21], thermal insulators [22], radomes [23], catalysts supports [24] and the like, radomes have drawn much attention recently, which are usually attached to the fore-end of a missile to protect them from the severe environment [25]. Considering their main feature for load bearing, wave transparent, thermal insulation and resistance to erosion, radome materials should possess high mechanical strength, low dielectric constant and loss tangent, low thermal conductivity, excellent thermal shock resistance and chemical stability and so on [26, 27]. It is well known that porous Si_3N_4 ceramics become the good candidate for wave-transparent materials due to their excellent mechanical, thermal and dielectric performance [28–30].

In this research, single-shell silica and fly ash hollow spheres are added into Si_3N_4 slurry as the pore-forming agents to fabricate high-performance porous Si_3N_4-based ceramics for the applications of radome. In order to further improve the performance of products, dispersant reaction method is exploited to realize the uniform dispersity of hollow spheres in the suspension and the following perfect combination between spheres and ceramic matrix during curing process. The microstructures, phase compositions, mechanical and dielectric properties of the obtained porous ceramics have been studied in this research.

Experimental

Materials

Si_3N_4 powder (Vesta Ceramics AB, Sweden; average particle diameter 0.30 μm, specific surface area

9.39 m^2/g), sintering additives including Al_2O_3 (99.9% purity, average particle size 0.25 μm, provided by Almatis, Ludwigshafen, Germany) and Y_2O_3 (99.95% purity, average particle size 0.39 μm, supplied by Shanghai Junyu Ceramic-molded Product Co., Ltd., China) were used as the main raw materials. Fly ash hollow microspheres (Jingsheng Minerals Co., Ltd., China) and silica hollow microspheres (Forsman Scientific (Beijing) Co., Ltd., China) were chosen as the single-shell hollow microspheres. Tetramethylammonium hydroxide aqueous solution (TMAOH, 10 wt%) as the dispersant and glycerol diacetate (GDA) as the coagulation agent were used to perform the dispersant reaction process, which were all purchased from Hengye Zhongyuan Chemical Co., Ltd., Beijing, China.

Preparation of porous Si_3N_4 ceramics with single-shell hollow microspheres

In a typical procedure of dispersant reaction method (as shown in Fig. 1), ceramic powders including Si_3N_4 powder, sintering additives (1 wt% Al_2O_3 and 2 wt% Y_2O_3, based on the mass of Si_3N_4 powder) and 0.2 wt% TMAOH (based on the mass of Si_3N_4 powder) were mixed with deionized water and then ball-milled for 12 h to achieve homogenous aqueous suspension. Subsequently, under the intense agitation, either fly ash hollow microspheres or silica hollow microspheres were introduced to the suspension, coupled with 3 vol.% GDA (based on the total volume of suspension) which was adopted as coagulation agent. The solid loadings of Si_3N_4 slurry and correspondingly additive amount of hollow microspheres are listed in Table 1. After degassing for 10 min, the slurry was immediately casted into a plastic mold coated with vaseline and then placed in water bath with temperature of 60 °C for 1 h, followed by demolding and drying in the oven at the temperature of 70 °C for 12 h. Finally, porous ceramics were fabricated by sintering green bodies at 1750 °C for 2 h under 0.5 MPa nitrogen atmosphere.

Characterization

The compositions and morphology of obtained products were characterized by X-ray diffraction using Cu Kα radiation (XRD, D8 ADVANCE, Bruker, Karlsruhe, Germany), X-ray fluorescence spectrograph (XRF-1800, Shimadzu, Kyoto, Japan) and scanning electron microscopy (SEM, MERLIN VP Compact, Carl Zeiss, Jena, Germany), respectively. Pore size distribution of porous ceramics is conducted via mercury porosimetry (Autopore IV 9510, Micromeritics Instrument Corp., Norcross, GA). The mechanical properties were tested by a universal material testing machine (AG2000G, Shimadzu, Japan). The dielectric constant was evaluated through the complex permittivity in the frequency range of 8.2–11.0 GHz, which was measured by a vector network analyzer (Agilent Technologies E8362B: 10 MHz–20 GHz) based on the waveguide method.

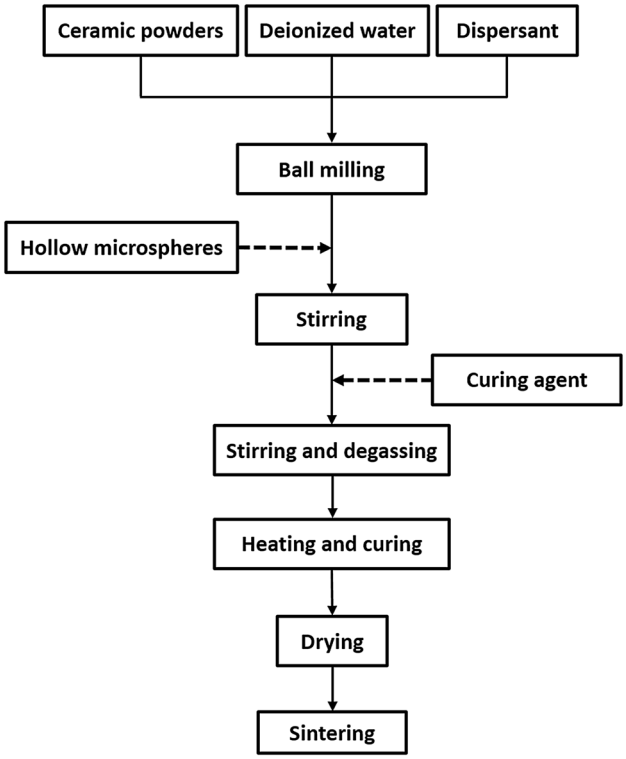

Figure 1 Flowchart of the preparation of porous ceramics via dispersant reaction method in combination with hollow microspheres as pore-forming agent.

Results and discussion

Phase composition and microstructure of hollow spheres

Figure 2 demonstrates the compositions and morphology of silica and fly ash hollow spheres. The microspheres chosen in this work were perfectly spherical. Obviously, from the cross-sectional morphology displayed in the insets of Fig. 2a, b, we can

Table 1 The detailed compositions of varied suspensions with different solid loadings or hollow microspheres

Type of hollow microsphere	Solid loading of Si_3N_4 slurry (vol.%)	Additive amount of hollow microspheres (wt%, based on the mass of Si_3N_4 powder)
SiO_2	32.5	28.32
SiO_2	35.0	22.64
SiO_2	37.5	13.09
SiO_2	40.0	8.04
Fly ash	40.0	7.15

see that both kinds of hollow spheres exhibit single-shell and well-defined hollow structure, which offers sufficient condition for the introduction of pores and subsequent reaction with the matrix. Figure 2c illustrates the diameters of hollow spheres. Both silica and fly ash hollow spheres abide to the normal distribution, which could make it easy to fabricate porous ceramics with high porosity through adding hollow spheres as pore-forming agents. The size of silica hollow spheres ranges from 6 to 70 μm and their median diameter is 24.47 μm, while the fly ash hollow spheres with larger size ranging from 20 to 160 μm possess median diameter of 68.90 μm. The phase compositions of the hollow spheres are shown in Fig. 2d. No sharp peaks are found in silica hollow spheres, indicating that they are composed of amorphous phase, while the fly ash hollow spheres mainly consist of mullite phase, which also corresponds to the XRF results shown in Table 2.

Microstructural properties

In this research, dispersant reaction method is employed, which utilizes the decrease in repulsive force between ceramic particles and hollow spheres resulting from the invalidation of dispersant. Figure 3a briefly describes the fabrication of porous ceramics from hollow spheres in combination with dispersant reaction method. Firstly, homogenous and well-dispersed suspension containing ceramic particles and hollow spheres is the crucial point for the

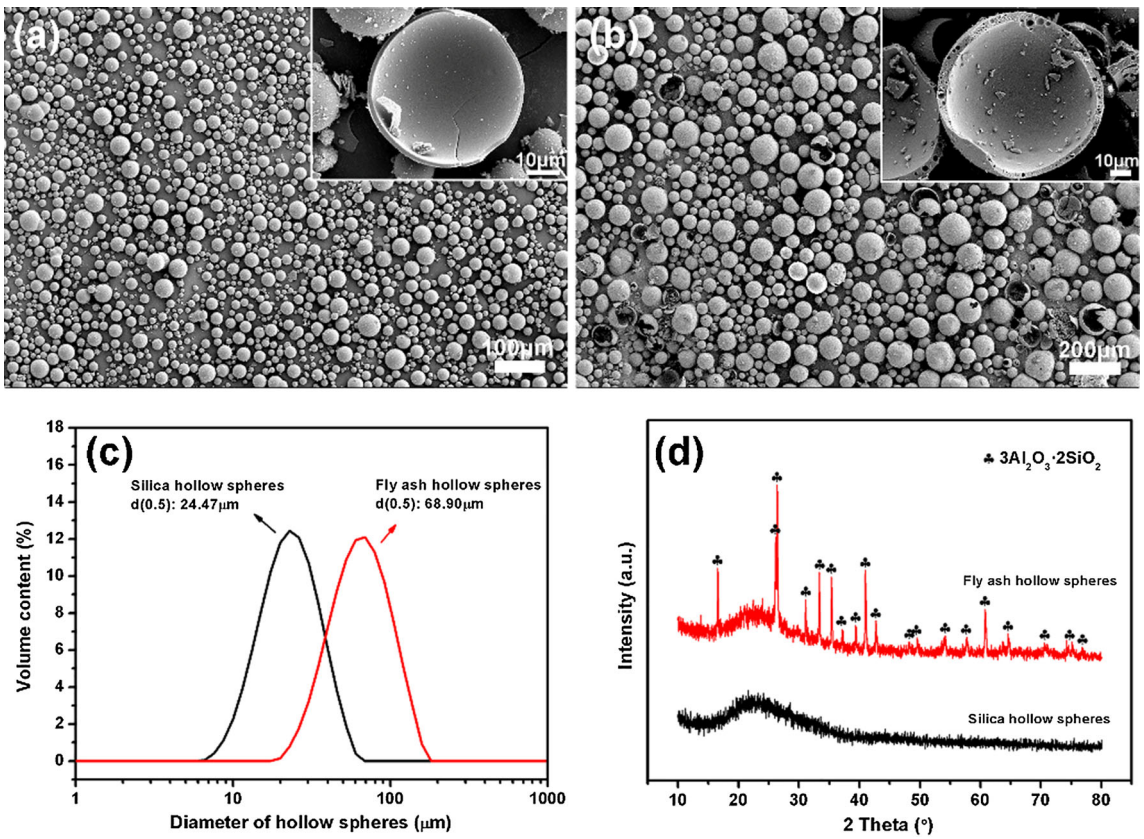

Figure 2 **a** SEM images of silica hollow spheres, **b** SEM images of fly ash hollow spheres, **c** diameter distribution of hollow spheres, **d** XRD patterns of hollow spheres.

achievement of porous ceramics with uniform pores, which could be achieved through selecting appropriate dispersant, that is the TMAOH. It could adsorb onto the surface of both ceramic particles and hollow spheres to endow them the repulsive forces between each other [31]. Afterward, the increase in temperature to 60 °C leads to the hydrolysis of curing agent (GDA), and then, acetic acid generates according to Eq. (1). The following acid–base neutralization reaction between acetic acid and TMAOH remarkably reduces the repulsion among ceramic particles and hollow spheres. As a result, green bodies with ceramic particles closely contacting hollow spheres can be obtained, which improves the better combination strength of the boundary between them. Consequently, the voids inside the hollow spheres provide the primary pores of porous ceramics. Figure 3b, c illustrates the morphology of green body and porous ceramics, respectively. It is clearly shown that silica hollow spheres uniformly distributed in the matrix are densely surrounded by the ceramic particles. After sintering, ceramic foams with hierarchical pore structure are prepared, and their pore size distribution with bimodal peaks demonstrates that porous ceramics possess two scale ranges of pore sizes, that is, smaller pores less than 2 μm correspond to the interlaced grains, and larger pores ranging from 2 to 10 μm evolve from the sintering reaction between the single-shell silica hollow spheres and matrix composed of ceramic particles.

$$(CH_3)_4NOH + CH_3COOH \rightarrow CH_3COON(CH_3)_4 + H_2O \quad (1)$$

For better regulating the porosity and performance of prepared porous ceramics, Si_3N_4 slurries with different solid loadings varying from 32.5 to 40.0 vol.% have been employed. Maximum silica hollow spheres that make the final suspension to satisfy high solid loading and casting-required viscosity simultaneously are added into the slurry. XRD patterns in Fig. 4 illustrate that Si_2N_2O is the dominant phase of porous ceramics when the solid loading of the initial Si_3N_4 slurry is as low as 32.5 vol.%, which is the product from the reaction between hollow spheres and matrix according to Eq. (2) [32]. Along with the increase in sintering temperature above 1500 °C, silica hollow spheres transformed into liquid due to their reaction with the sintering aids, i.e., Al_2O_3 and Y_2O_3. Afterward, the sintering temperature keeps rising to the target temperature 1750 °C, meanwhile the dissolution of α-Si_3N_4 and the reprecipitation of β-Si_3N_4 occur. Si_2N_2O phase generates from the reaction between β-Si_3N_4 and liquid phase, leading to the densification and decrease in liquid phase. However, the less silica hollow spheres make remarkable β-Si_3N_4 phase left, which can be proved by the fact that the peaks belonging to β-Si_3N_4 are slightly lower than those of Si_2N_2O. As the relative amount of Si_3N_4 increases, the intensity of Si_2N_2O decreases. When the solid loading of the initial Si_3N_4 slurry reaches 40.0 vol.%, due to the decrease in additive amount of SiO_2 hollow microspheres, SiO_2 source decreases while Si_3N_4 source increases. Based on Eq. (2), very little Si_2N_2O is formed in the porous ceramics. Considering the sintering temperature of 1750 °C, massive residual α-Si_3N_4 transformed into β-Si_3N_4, making β-Si_3N_4 to be the main phase.

$$Si_3N_4(s) + SiO_2(s) = 2Si_2N_2O(s) \quad (2)$$

Mechanical properties

Higher solid loading of the initial Si_3N_4 slurry indicates that less amount of silica hollow spheres are added. As a consequence, the bulk density of porous ceramics increases gradually from 1.04 to 1.43 g/cm^3, while their open porosity decreases from 64.83 ± 0.49% to 54.36 ± 0.50% (see Fig. 5a), obviously indicating the significant pore-forming role of single-shell silica hollow spheres. Influenced by the phase composition and microstructure, the mechanical properties are improved with the increase in solid loading of the initial Si_3N_4 slurry. The flexural strength of porous ceramics varies from 33.10 ± 0.36 to 64.01 ± 3.08 MPa, while their fracture toughness increases from 0.56 ± 0.01 to 1.03 ± 0.06 MPa m$^{1/2}$ (see Fig. 5b).

Table 2 Compositions of fly ash hollow microspheres

Compound	SiO_2	Al_2O_3	CaO	Fe_2O_3	K_2O	TiO_2	Na_2O	MgO
Content (wt%)	55.02	38.02	1.86	1.46	1.32	0.67	0.56	0.56

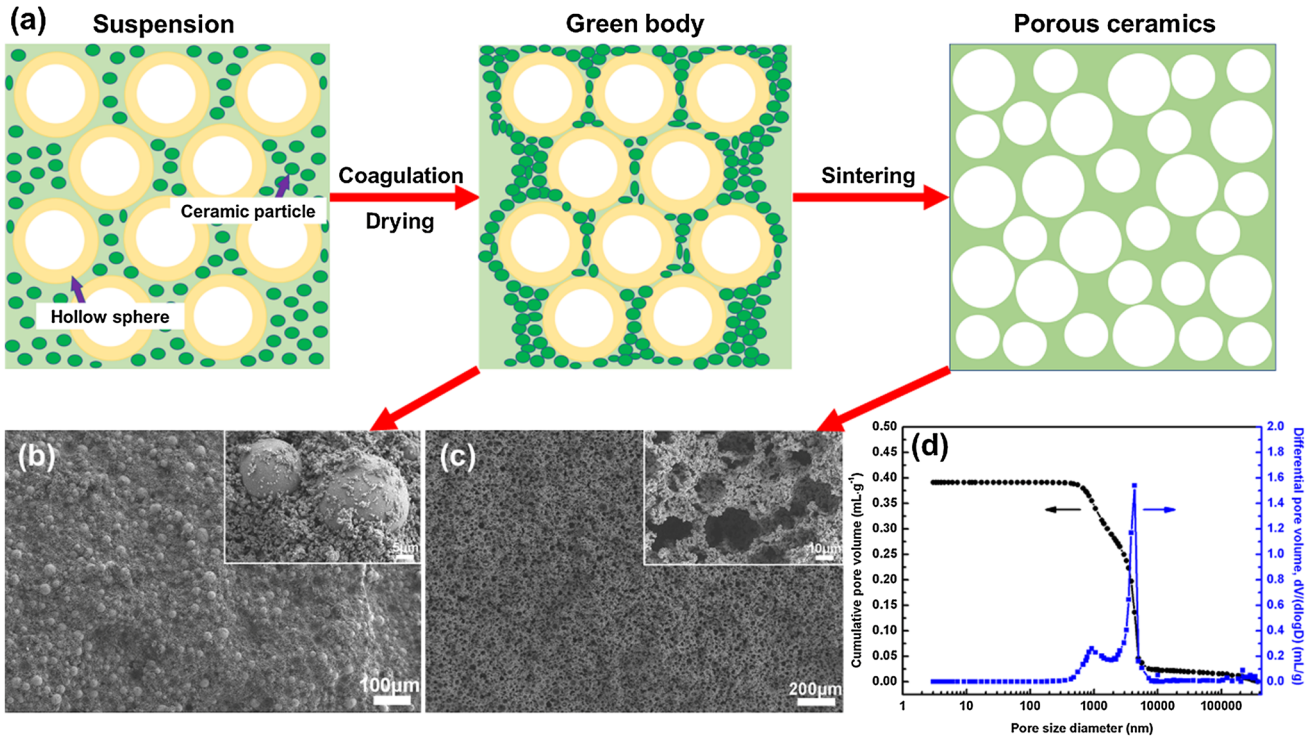

Figure 3 **a** Schematic diagram of the fabrication process of hollow sphere ceramics, SEM images of **b** green body and **c** porous ceramics and their pore size distribution **d** (prepared with 35.0 vol.% Si_3N_4 slurry and addition of 22.64 wt% silica hollow microspheres).

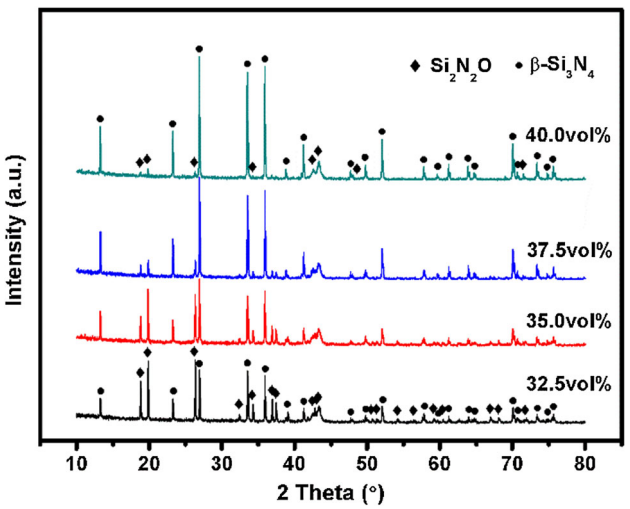

Figure 4 XRD patterns of porous ceramics with addition of silica hollow microspheres.

Dielectric properties

As one of the main inorganic materials applied in the radome [30], the dielectric constant of porous Si_3N_4-based ceramics is investigated here as shown in Fig. 6. For radome materials, one of the most significant performances is the wave-transparent property to ensure the transmission of electromagnetic signals, which is determined by the dielectric constant. Thus, within a certain band range, porous ceramics with low and stable dielectric constant (< 4.0) are promising to be applied as the radome materials. Moreover, as demonstrated by many researches, porosity and phase composition are the two major factors determining the dielectric properties [33]. Due to the excellent dielectric properties of Si_2N_2O ceramic with dielectric constant of 4.80 [35], as well as the lower bulk density of the samples prepared from 32.5 vol.% Si_3N_4 slurry, the obtained porous Si_2N_2O-Si_3N_4 ceramics exhibit outstanding dielectric constant of 2.27. Although the increase in bulk density and amount of β-Si_3N_4 with relatively high dielectric constant of 7.96 [26] brings negative effect on the dielectric properties, porous Si_3N_4-based ceramics from even higher solid loading of Si_3N_4 slurry possess dielectric constant of 2.89. Moreover, in the wide range of frequency from 8.2 to 11.0 GHz, the dielectric constant of all specimens shows stable trend, which further indicates that they are ideal for radome application.

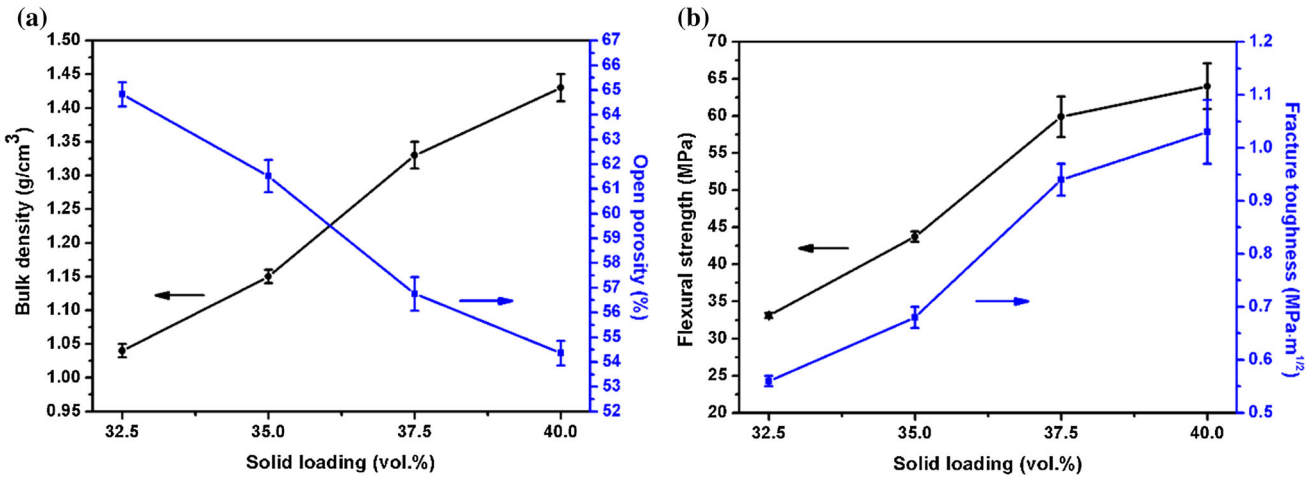

Figure 5 **a** Bulk density and open porosity **b** flexural strength and fracture toughness of porous ceramics with addition of silica hollow microspheres.

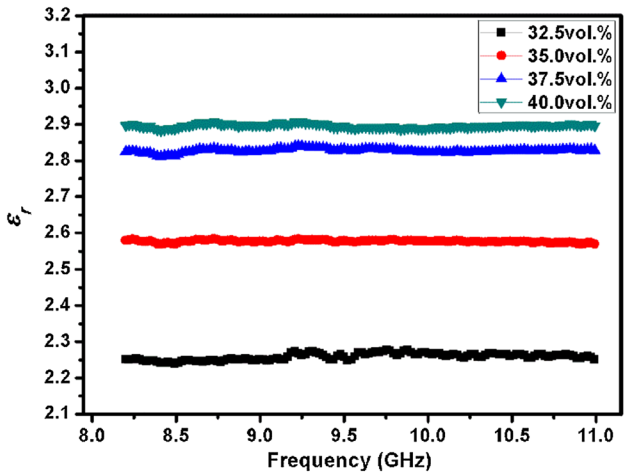

Figure 6 Dielectric constant as a function of frequency in the range of 8.2–11.0 GHz.

Properties of porous ceramics from fly ash hollow spheres

In order to further enhance the mechanical properties of the porous ceramics, another kind of hollow microspheres, namely fly ash hollow microspheres, has been introduced into the relatively high solid-loading Si_3N_4 slurry (40.0 vol.%). The morphology of prepared green body is present in Fig. 7a. Benefited from the dispersant reaction method, fly ash hollow spheres scatter uniformly in the matrix and they are coated by lots of ceramic particles. After sintering process, interior voids in hollow spheres transform to pores, and rod-like grains are generated from ceramic particles to make up skeleton of porous ceramics, as shown in Fig. 7b. Therefore, multi-scale pore structure constituted by primary macropores and porous rod-assembled strut is generated. Pore size distribution shown in Fig. 7c illustrates that the median pore diameter of the porous ceramics is concentrated at 780 nm, which could be ascribed to the partial sintering. Although fly ash hollow microspheres are mainly composed by SiO_2 and Al_2O_3 (see Table 2), the additive amount is relatively low with respect to the content of Si_3N_4 in the slurry. Thus, fly ash hollow microspheres would firstly melt and then react with surrounded Si_3N_4 with little phase transformation. XRD patterns demonstrated that porous Si_3N_4 ceramics are fabricated here (see Fig. 7d).

Based on the results about effects of silica hollow microspheres, it is obvious to find that the increase in solid loading leads to the decreasing addition of hollow microspheres, further making the decrease in porosity and improvement in both mechanical and dielectric properties. For fly ash hollow microspheres, relatively high solid loading (40 vol.%) is chosen here aiming at fabricating high-performance porous ceramics. Compared with silica hollow microspheres, fly ash hollow microspheres possess larger diameter, making their additive amount to decrease slightly. It is found that in the case of same initial slurry, porous

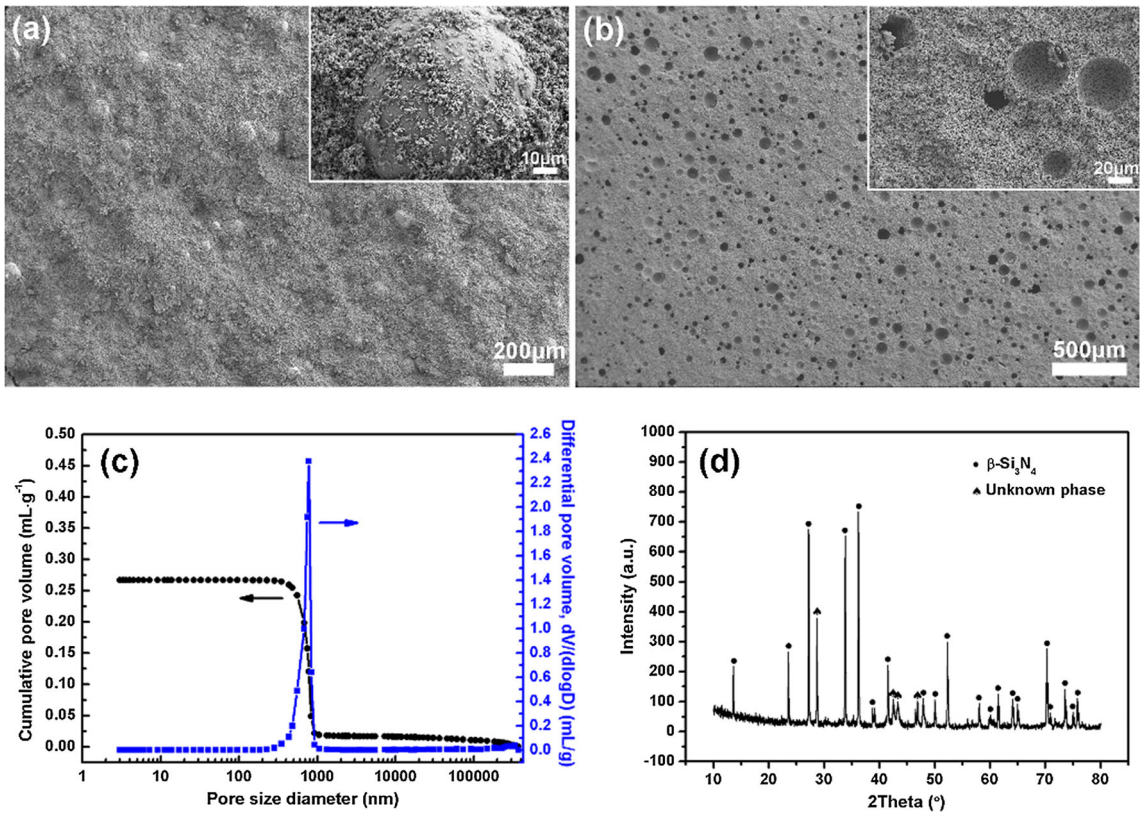

Figure 7 SEM images of **a** green body and **b** porous ceramics with addition of fly ash hollow microspheres, **c** pore size distribution and **d** XRD pattern of porous ceramics (prepared with 40.0 vol.% Si_3N_4 slurry and addition of 7.15 wt% fly ash hollow microspheres).

Si_3N_4 ceramics with higher bulk density of 1.73 g/cm^3 are achieved, leading to higher flexural strength of 108.76 ± 6.25 MPa and fracture toughness of 1.78 ± 0.09 MPa m$^{1/2}$ as well as dielectric constant of 3.53. Due to the increase in particle size for fly ash hollow microspheres, the content of introduced pores decreases, further leading to the decrease in porosity of the final porous Si_3N_4 ceramics. On the other hand, the only phase in porous Si_3N_4 ceramics is β-Si_3N_4, while there are β-Si_3N_4 and little Si_2N_2O in the porous ceramics from silica hollow microspheres and 40 vol.% the initial Si_3N_4 slurry. As discussed before, Si_2N_2O possesses lower mechanical strength and dielectric constant than Si_3N_4. As a result, porous Si_3N_4 ceramics from fly ash hollow microspheres show better mechanical properties and relative high dielectric constant, which still meets the requirement for radomes [25].

The performance superiority of porous Si_3N_4 ceramics from this method is well reflected through the comparison in Table 3. The addition of silica hollow microspheres favors porous Si_3N_4 ceramics with excellent dielectric property, which can be well explained by the uniform pore size distribution and small pore size. Moreover, altering the species of pore former could significantly improve the mechanical properties of porous ceramics, owing to the small amount of alumina in the low-cost fly ash hollow microspheres. Obviously, even with higher porosity, superior flexural strength and dielectric constant are achieved by adding fly ash hollow microspheres when compared with that from freeze-drying. The employment of single-shell hollow microspheres with good sphericity and diameter uniformity as pore source, in combination with low-cost, eco-friendly, high-efficiency and versatile dispersant reaction method, promotes the controllable fabrication of high-performance porous ceramics with uniform micropores.

Table 3 Performance comparison of porous Si_3N_4-based ceramics fabricated from various methods

Method	Pore source	System	Porosity (%)	Flexural strength (MPa)	Dielectric property	
					Frequency (GHz)	Dielectric constant
Gelcasting-pressureless sintering	Binder removal and overlapped rod-like β-Si_3N_4	SNNWs/Si_3N_4 [34]	40.7	84.3	8–12	3.6–3.8
		Si_3N_4 [30]	39.3	146	14.0	4.03
		Si_3N_4-Si_2N_2O [32]	24.5	170	12.4–18.0	4.76
		Si_3N_4-Si_2N_2O [35]	47.3	68.7	14	3.4
Freeze-drying	Freezing medium and overlapped rod-like β-Si_3N_4	Si_3N_4 [36]	40.6	94.7	12.5	3.7
Freeze-drying combining with oxidation sintering	Pores among ceramic particles	Si_3N_4 [23]	21.5	71–74	14	3.4–3.6
Adding pore-forming agents method	$(NH_4)_2HPO_4$	Si_3N_4-Si_2N_2O-BN [34]	51.0	75	21	3.52
	PMMA microspheres	ZrO_2-SiO_2 aerogels-Si_3N_4 [37]	62.6	53.86	12.15	2.86
	Diatomite	SiO_2-Si_3N_4 [38]	50.1	78.04	27	2.95
Present work	Silica hollow microspheres	Si_2N_2O-Si_3N_4	56.6	64.01	10.0	2.89
		Si_3N_4	66.1	33.10	10.0	2.27
	Fly ash hollow microspheres	Si_3N_4	45.7	108.76	10.0	3.53

Conclusions

A kind of non-toxic, highly efficient, versatile direct coagulation casting method, namely dispersant reaction, has been employed to form green bodies containing hollow microspheres and ceramic particles. Different from other pore formers, the unique single-shell structure of hollow microspheres provides enough space to form primary pores during sintering process, and it makes the morphology of products more controllable. Moreover, uniform diameter distribution of hollow microsphere and the obtained hierarchical pore structure becomes one of the reasons explaining their high performances. The addition of silica hollow microspheres facilitates the fabrication of high-performance porous Si_2N_2O-Si_3N_4 ceramics with excellent dielectric constant varying from 2.27 to 2.89. Besides, when fly ash hollow microspheres are added, high-performance porous Si_3N_4 ceramics with porosity of 45.7%, flexural strength of 108.76 MPa and dielectric constant of 3.53 have been achieved, which could be one of the ideal candidates for radomes.

Acknowledgements

This work was supported by the National Natural Science Foundation of China (Grant Nos. 51572140 and 51702184) and China Postdoctoral Science Foundation (Grant Nos. 2018M630154, 2018M630149 and 2018M631492).

Compliance with ethical standards

Conflict of interest This contribution has been approved by all coauthors, it has not been published before, it is not under consideration for publication anywhere else, and there is no conflict of interest.

References

[1] Zhang J, Wang G, Jin F, Fang X, Song C, Guo X (2013) Fabrication of hollow spheres by dry-gel conversion and its application in the selective hydrodesulfurization of FCC gasoline. J Colloid Interface Sci 396:112–119

[2] Ma N, Deng Y, Liu W, Li S, Xu J, Qu Y, Gan K, Sun X, Yang J (2016) A one-step synthesis of hollow periodic

mesoporous organosilica spheres with radially oriented mesochannels. Chem Commun 52:3544–3547

[3] Li W, Gao R, Chen M, Zhou S, Wu L (2013) Facile synthesis and unique photocatalytic property of niobium pentoxide hollow spheres and the high optoelectronic performance of their nanofilm. J Colloid Interface Sci 411:220–229

[4] Li B, Yang Y, Li B, Liu Q, Zhang Y, Zhang N, Du X (2013) Low temperature synthesis of hollow $La_2Mo_2O_9$ spheres by the molten salt solvent method. CrystEngComm 15:6905–6910

[5] Kang N, Park JH, Jin M, Park N, Lee SM, Kim HJ, Kim JM, Son SU (2013) Microporous organic network hollow spheres: useful templates for nanoparticulate Co_3O_4 hollow oxidation catalysts. J Am Chem Soc 135:19115–19118

[6] Shao Y, Jia D, Liu B (2009) Characterization of porous silicon nitride ceramics by pressureless sintering using fly ash cenosphere as a pore-forming agent. J Eur Ceram Soc 29:1529–1534

[7] Huo W, Zhang X, Chen Y, Lu Y, Liu J, Yan S, Wu JM, Yang J (2018) Novel mullite ceramic foams with high porosity and strength using only fly ash hollow spheres as raw material. J Eur Ceram Soc 38:2035–2042

[8] Colombo P (2006) Conventional and novel processing methods for cellular ceramics. Philos Trans R Soc A Math Phys Eng Sci 364:109–124

[9] Zhang XY, Lan T, Li N, Wu JM, Huo WL, Ma N, Yang JL (2016) Porous silica ceramics with uniform pores from the in situ foaming process of silica poly-hollow microspheres in inert atmosphere. Mater Lett 182:143–146

[10] Sun Z, Lu C, Fan J, Yuan F (2016) Porous silica ceramics with closed-cell structure prepared by inactive hollow spheres for heat insulation. J Alloy Compd 662:157–164

[11] Geng H, Hu X, Zhou J, Xu X, Wang M, Guo A, Du H, Liu J (2016) Fabrication and compressive properties of closed-cell alumina ceramics by binding hollow alumina spheres with high-temperature binder. Ceram Int 42:16071–16076

[12] DeFriend KA, Barron AR (2003) A simple approach to hierarchical ceramic ultrafiltration membranes. J Membr Sci 212:29–38

[13] Qi F, Xu X, Xu J, Wang Y, Yang J, Colombo P (2014) A novel way to prepare hollow sphere ceramics. J Am Ceram Soc 97:3341–3347

[14] Qu YN, Xu J, Su ZG, Ma N, Zhang XY, Xi XQ, Yang JL (2016) Lightweight and high-strength glass foams prepared by a novel green spheres hollowing technique. Ceram Int 42:2370–2377

[15] Wu JM, Zhang XY, Yang JL (2014) Novel porous Si_3N_4 ceramics prepared by aqueous gelcasting using Si_3N_4 poly-hollow microspheres as pore-forming agent. J Eur Ceram Soc 34:1089–1096

[16] Khodaei M, Meratian M, Savabi O, Razavi M (2016) The effect of pore structure on the mechanical properties of titanium scaffolds. Mater Lett 171:308–311

[17] Chen F, Cao F, Pan H, Wang K, Shen Q, Li J, Wang S (2012) Mechanical and dielectric properties of silicon nitride ceramics with high and hierarchical porosity. Mater Design 40:562–566

[18] Lurie SA, Solyaev YO, Rabinskiy LN, Polyakov PO, Sevostianov I (2017) Mechanical behavior of porous Si_3N_4 ceramics manufactured with 3D printing technology. J Mater Sci 53:4796–4805. https://doi.org/10.1007/s10853-017-1881-0

[19] Pia G, Casnedi L, Sanna U (2016) Porosity and pore size distribution influence on thermal conductivity of yttria-stabilized zirconia: experimental findings and model predictions. Ceram Int 42:5802–5809

[20] Bakarič T, Rojac T, Abellard AP, Malič B, Levassort F, Kuscer D (2016) Effect of pore size and porosity on piezoelectric and acoustic properties of $Pb(Zr_{0.53}Ti_{0.47})O_3$ ceramics. Adv Appl Ceram 115:66–71

[21] Kumar A, Mohanta K, Kumar D, Parkash O (2015) Low cost porous alumina with tailored gas permeability and mechanical properties prepared using rice husk and sucrose for filter applications. Micropor Mesopor Mater 213:48–58

[22] Su L, Wang H, Niu M, Fan X, Ma M, Shi Z, Guo SW (2018) Ultralight, recoverable and high-temperature-resistant SiC nanowire aerogel. ACS Nano 12:3103–3111

[23] Cai Y, Li X, Dong J (2014) Properties of porous Si_3N_4 ceramic electromagnetic wave transparent materials prepared by technique combining freeze drying and oxidation sintering. J Mater Sci 25:1949–1954. https://doi.org/10.1007/s10854-014-1827-0

[24] Kawaguchi K, Suzuki Y, Goto T, Cho SH, Sekino T (2018) Homogeneously bulk porous calcium hexaaluminate ($CaAl_{12}O_9$): reactive sintering and microstructure development. Ceram Int 44:4462–4466

[25] Kandi KK, Thallapalli N, Chilakalapalli SPR (2015) Development of silicon nitride-based ceramic radomes-A review. Int J Appl Ceram Technol 12:909–920

[26] Ganesh I (2011) Development of β-SiAlON based ceramics for radome applications. Process Appl Ceram 5:113–138

[27] Wang Y, Liu J (2009) Aluminum phosphate-mullite composites for high-temperature radome applications. Int J Appl Ceram Technol 6:190–194

[28] Xiao S, Mei H, Han D, Yuan W, Cheng L (2018) Porous (SiC_w-Si_3N_{4w})/(Si_3N_4-SiC) composite with enhanced mechanical performance fabricated by 3D printing. Ceram Int 44:14122–14127

[29] Mei H, Zhao G, Liu G, Wang Z, Cheng L (2015) Effect of pore size distribution on the mechanical performance of

carbon foams reinforced by in situ grown Si_3N_4 whiskers. J Eur Ceram Soc 35:4431–4435

[30] Yang X, Li B, Zhang C, Wang S, Liu K, Zou C (2016) Fabrication and properties of porous silicon nitride wave-transparent ceramics via gel-casting and pressureless sintering. Mater Sci Eng A 663:174–180

[31] Gan K, Xu J, Zhang X, Huo W, Yang M, Qu Y, Yang J (2016) Direct coagulation casting of silicon nitride suspension via a dispersant reaction method. Ceram Int 42:4347–4353

[32] Lee SJ, Baek S (2016) Effect of SiO_2 content on the microstructure, mechanical and dielectric properties of Si_3N_4 ceramics. Ceram Int 42:9921–9925

[33] Wang S, Yang Z, Duan X, Jia D, Ma F, Sun B, Zhou Y (2014) Fabrication and characterization of in situ porous Si_3N_4-Si_2N_2O-BN ceramic. Int J Appl Ceram Technol 11:832–838

[34] Li D, Li B, Yang X, Guo S, Zheng Y (2018) Fabrication and properties of in situ silicon nitride nanowires reinforced porous silicon nitride (SNNWs/SN) composites. J Eur Ceram Soc 38:2671–2675

[35] Yang X, Li B, Zhang C, Wang S, Liu K, Zou C (2016) Design and fabrication of porous Si_3N_4-Si_2N_2O in situ composite ceramics with improved toughness. Mater Design 110:375–381

[36] Li L, Li Q, Hong J, Sun M, Zhang J, Dong S (2018) Effect of Si_3N_4 solid contents on mechanical and dielectric properties of porous Si_3N_4 ceramics through freeze-drying. J Alloy Compd 732:136–140

[37] Sun Y, Zhao Z, Li X (2018) A novel aerogels/porous Si_3N_4 ceramics composite with high strength and improved thermal insulation property. Ceram Int 44:5233–5237

[38] You G, Bi J, Chen Y, Yin C, Wang C (2016) Effect of diatomite additive on the mechanical and dielectric properties of porous SiO_2-Si_3N_4 composite ceramics. J Wuhan Univ Technol 31:528–532